Contents lists available at ScienceDirect

Digital Chinese Medicine

journal homepage: http://www.keaipublishing.com/dcmed

Protective effects of Fufang Ejiao Jiang against aplastic anemia assessed by network pharmacology and metabolomics strategy

HE Dan, ZHANG Haichao, YI Ziyang, ZHAO Di, ZHANG Shuihan*

Hunan academy of Chinese Medicine, Hunan University of Chinese Medicine Changsha, Hunan 410013, China

ARTICLE INFO

Article history
Received 19 July 2021
Accepted 14 November 2021
Available online 25 December 2021

Keywords
Fufang Ejiao Jiang (复方阿胶浆，FFEJJ)
Aplastic anemia
Network pharmacology
Metabolomics
Lipid metabolomics
Hematopoiesis microenvironment
Acetylphenylhydrazine
Cetylphenylhydrazine

*Corresponding author: ZHANG Shuihan, Professor. Research drection: traditional Chinese medicine resources.
E-mail: zhangshuihan0220@126.com.

Peer review under the responsibility of Hunan University of Chinese Medicine.

ABSTRACT

Objective To elucidate the mechanisms underlying the therapeutic effects of Fufang Ejiao Jiang (复方阿胶浆，FFEJJ) on aplastic anemia (AA) using integrated network pharmacology and serum metabolomics.

Methods Traditional Chinese Medicine Systems Pharmacology (TCMSP), Pubmed, integrative pharmacology-based research platform of traditional Chinese medicine (TCMIP), and Bioinformatics Analysis Tool for Molecular mechANism of Traditional Chinese Medicine (BATMAN-TCM) were used to identify the constituents and putative targets of FFEJJ. GeneCards and DisGeNET databases were used to identify AA-associated targets. We constructed a herb-component-target network and analyzed the protein-protein interaction (PPI) network. Potential mechanisms were determined using Kyoto Encyclopedia of Genes and Genomes (KEGG) pathway enrichment analyses. In addition, an AA model was established using acetylphenylhydrazine (APH) and cetylphenylhydrazine (CTX). Ultra-performance liquid chromatography-quadrupole time-of-flight mass spectrometry (UPLC-Q-TOF/MS)-based serum metabolomics was applied to screen potential metabolites and the related pathways associated with AA and the potential anti-anemic effects of FFEJJ.

Results A total of 30 active components of FFEJJ and 24 targets were related to AA. PPI network analysis showed that VEGFA, AKT1, IL-6, CASP3, and ICAM1 were key nodes overlapping with proteins known to be related to AA. KEGG pathway enrichment analysis revealed that the presumed targets of FFEJJ were mainly associated with pathways linked to the promotion of hematopoiesis and improvement of the hematopoietic microenvironment. A total of 423 metabolite biomarkers were identified between the control and AA models, which are involved in the development of AA. In contrast, FFEJJ reversed the 79 differential metabolites altered by AA. Pathway analysis suggested that the synergistic effects of FFEJJ were mainly enriched in 24 metabolic

pathways. Among them, sphingolipid metabolism, glycerophospholipid metabolism, and arachidonic acid metabolism were related to promoting hematopoiesis and improving the hematopoietic microenvironment, which partially conforms with network pharmacology. The interaction network formed by three key differential metabolites, including hydroxy-eicosatetraenoic acid (HETE), sphingosine 1-phosphate (S1P), and lysophosphatidylcholine (lysoPC), and three predicted network targets (VEGFA, CASP3, and ICAM1) may be the potential mechanism underlying the anti-AA action of the multi-component of FFEJJ.

Conclusion FFEJJ could be an alternative treatment option for AA. It acts by promoting hematopoiesis and improving the hematopoietic microenvironment. Network pharmacology-integrated metabolomics makes it possible to analyze TCMs from a systems perspective and at the molecular level.

DOI: 10.1016/j.dcmed.2021.12.007
Citation: HE D, ZHANG HC, YI ZY, et al. Protective effects of Fufang Ejiao Jiang against aplastic anemia assessed by network pharmacology and metabolomics strategy. Digital Chinese Medicine, 2021,4(4): 328–342.

1 Introduction

Aplastic anemia (AA) is a hematological disorder with subtle onset caused by various factors. Bone marrow hematopoietic failure is the main clinical manifestation of this condition [1]. Moreover, it is responsible for high morbidity and mortality in the Asian population [2-4]. Although frontline therapies such as immunosuppressive therapy (IST) and bone marrow transplantation (BMT) have been applied in the last decade, side effects and recurrence rates remain high [5]. Thus, it is necessary to develop new and effective therapeutic strategies for AA. In addition, due to the multiple pathological mechanisms of AA, combination treatments instead of monotherapy should be considered.

Traditional Chinese medicine (TCM), particularly the TCM formula with multiple herbs, has become an important factor in the treatment and prevention of AA [6]. According to TCM, AA is a physical condition that lacks Qi and blood. Fufang Ejiao Jiang (复方阿胶浆, FFEJJ) is characterized as having therapeutic efficacy against leukopenia and anemia, consisting of five herbs: Ejiao (Asini Corii Colla), Hongshen (Ginseng Radix et Rhizoma Rubra), Shudihuang (Rehmanniae Radix Preparata), Dangshen (Codonopsis Radix), and Shanzha (Crataegi Fructus). It is a commonly used prescription for “nourishing Qi and nourishing blood”. Previous studies have shown that FFEJJ alleviates myelosuppression by increasing the proliferation of hematopoietic stem cells (HSCs) and improving the bone marrow microenvironment [7, 8]. However, the therapeutic mechanism of FFEJJ in AA still needs further investigation to promote progress in the clinical application and development of FFEJJ.

Recently, network pharmacology combined with metabolomics has been widely employed to explore the molecular mechanisms of TCM at a holistic level. Several studies have indicated that network pharmacology enables the identification of drug-gene-disease co-module associations in a high-throughput manner [9-11]. Furthermore, its "network target, multi-components" is relatively consistent with the synergistic multi-compound characteristics of TCM. Metabonomics study plays an important role in comprehensively surveying the endogenous metabolites of the organism or organ and their relationship with internal or extrinsic factors. This combination is powerful for identifying the active components and mechanisms of action of TCMs.

In this study, network pharmacology was applied to identify the potential bioactive components in FFEJJ and elucidate its therapeutic mechanisms in AA. The metabolomics method was used to monitor alterations in endogenous substances after treatment with FFEJJ, aiming for an experimental gist associated with the metabolic mechanism of FFEJJ in AA. We performed network pharmacology and metabolomics analysis to elucidate the molecular mechanism of FFEJJ in AA.

2 Materials and methods

2.1 Database and software

(1) Herbs and components database: Traditional Chinese Medicine Systems Pharmacology Database

and Analysis Platform (TCMSP, http://lsp.nwu.edu.cn/tcmsp.php, ver.2.3), PubMed (https://www.ncbi.nlm.nih.gov/pubmed), Integrative Pharmacology-based Research Platform of Traditional Chinese Medicine (TCMIP, v2.0, http://www.tcmip.cn), and Bioinformatics Analysis Tool for Molecular mechANism of Traditional Chinese Medicine (BATMAN-TCM, http://bionet.ncpsb.org.cn/batman-tcm/). (2) Disease databases: GeneCards database (https://www.genecards.org/ ver.5.2) and the DisGeNET database (http://www.disgenet.org, last update: May 2020). (3) Protein database UniProt database (http://www.rcsb.org/). (4) Network visualization database and software: STRING online database (https://string-db.org/), Cytoscape 3.7.2 software, and OmicShare cloud platform (http://www.omicshare.com). (5) Enrichment database: Database for Annotation, Visualization, and Integrated Discovery (DAVID) platform (https://david.ncifcrf.gov/) and MetaboAnalyst (https://www.metaboanalyst.ca/MetaboAnalyst/, ver.5.0). (6) Metabolite identification database: Human Metabolome Database (HMDB, http://www.hmdb.ca/), METLIN (http://metlin.scripps.edu).

2.2 Network pharmacology analysis

2.2.1 The prediction of potential targets for FFEJJ and AA Based on the TCMSP database, the active components and targets of FFEJJ were identified based on oral bioavailability (OB ⩾ 30%) and drug-like (DL ⩾ 0.18) characteristics. GeneCards and DisGeNet databases were employed to obtain the AA-correlated therapeutic targets, and the keywords were set as “aplastic anemia” and “Homo sapiens”.

2.2.2 Enrichment analysis Gene Ontology (GO) function and Kyoto Encyclopedia of Genes and Genomes (KEGG) enrichment analysis were performed on the DAVID platform. The species was also set as “Homo sapiens”. The OmicShare cloud platform was used to visualize the histograms and bubble map charts.

2.2.3 Construction of network The component-targets-pathway network was established and visualized using Cytoscape 3.7.2 software. A protein-protein interaction (PPI) network was constructed using STRING. Topological parameters [including the degree and betweenness centrality (BC)] of the node were calculated to identify hub components, key targets, and pathways.

2.3 Metabolic analysis

2.3.1 Animal experiments Twenty-one male specific pathogen-free (SPF) grade Sprague-Dawley (SD) rats aged eight weeks weighing 200 – 220 g were purchased from Hunan SJAC Laboratory Animal Co., Ltd. (No. 43004700058820). Before the experiment, animals were adaptively maintained and housed for one week in a SPF-grade facility at Hunan Academy of Chinese Medicine (License No. SYXK [Xiang] 2020-0008). All animal experiments were performed in accordance with the protocols and guidelines approved by the Animal Ethics Committee of the Hunan Academy of Chinese Medicine (Approval No. 20190041).

After adaptation, the SD rats were randomized into three groups: control group (n = 7), model group (n = 7), and FFEJJ treatment group at a dose of 5.4 mL/kg (n = 7) [12]. On the 8th day of drug administration, the model and FFEJJ groups received an intraperitoneal injection of 30 mg/kg, 1-acetyl-2-phenylhydrazine (APH). On the 12th day, 100 mg/kg cyclophosphamide (CTX) + APH was injected [13]. The control group was injected equal amounts of normal saline and distilled water. All the rats were euthanized after drug treatment. In a previous study, histological examination and peripheral blood (PB) routine tests were applied to evaluate the quantity of blood cells and the AA model [12] (Figure 1).

2.3.2 Sample collection and preparation The following procedures were used to determine serum metabolism. First, 100 μL serum samples were thawed at 4 °C for 30 min. 300 μL pre-cooling mixture of methanol and acetonitrile (2/1, v/v) was added to the sample to completely remove the protein. In addition, 10 μL internal standard (0.3 mg/mL 2-chloro-l-phenylalanine (HPLC ⩾ 98%, Adamas-beta) was also dispersed in this mixture. Thereafter, they were vortexed for 30 s. Subsequently, the above mixture was continued at 13 000 rpm and 4 °C for 15 min. The supernatant was filtered through a microfilter (0.22 μm). Finally, 10 μL supernatant was detected by ultra-performance liquid chromatography-quadrupole time-of-flight mass spectrometry (UPLC-QTOF/MS). All samples were maintained at 4 °C prior to analysis.

Before sample preparation, quality control (QC) was prepared using an equal volume (100 μL) of samples from each group to evaluate the repeatability of the experimental methods and ensure the reliability of the metabolomic data. In our study, one QC sample was inserted into every six samples. Moreover, some ions were removed when their relative abundance was less than 30% of the QC.

2.3.3 UHPLC-MS analysis Serum metabolic profiles were obtained using a UPLC-QTOF/MS system in positive and negative ESI ion modes. An ACQUITY UPLC BEH C18 column (100 mm × 2.1 mm, 1.7 μm,

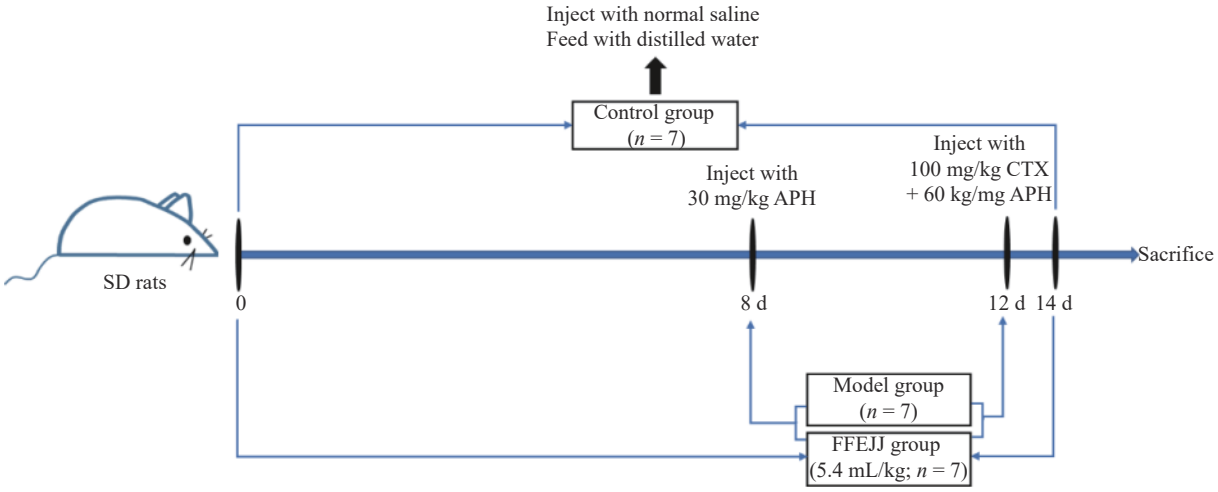

Figure 1 Animal experiments flow chart

Waters, USA) was used to optimize the gradient elution. In addition, 0.1 % formic acid water (A) and methanol (B) were used as the mobile phases. The working process is as follows: 0.01 – 1.5 min, 5% B; 1.5 – 3 min, 5% – 30% B; 3 – 7 min, 30% – 60% B; 7 – 9 min, 60% – 90% B; 9 – 11 min, 90% – 100% B; 11 – 12 min, 100% B; 12 – 15 min, 100% – 5% B. The injection volume, flow rate column, and temperature were 10 μL, 0.35 mL/min, and 45 °C, respectively. The following are the mass spectrum parameters for this experiment: the ion source temperature was set at 320 °C (+) and 320 °C (–); ion spray voltage was 3 500 V (+) and 3 100 V (–); curtain gas, 30 PSI; mass scan, 60 – 900 (+) and 60 – 900 (–); and collision energy was 30 eV.

2.3.4 Identification and quantitative analysis Prognosis QI software (Waters Corporation, Milford, USA) was used to calibrate the peak, including alignment, peak picking, and deconvolution [14]. Based on the human metabolome database (HMDB) and a metabolite mass spectral database (METLIN), metabolites were identified according to the characteristic rule of retention time (RT), m/z, and the ionic fragments of MS/MS results [15, 16]. The relative content of each metabolite was calculated by comparing the relative peak areas of the internal standard samples. The identification of biomarkers was enriched on the MetaboAnalyst platform.

2.4 Multivariate statistical analysis

A *t* test was used to identify significantly changed metabolites. Hierarchical cluster analysis (HCA) and orthogonal partial least squares discriminant analysis (OPLS-DA) were employed to distinguish different groups (model group, control group, and FFEJJ group) [17, 18]. Potential biomarkers were required to meet the variable importance projection (VIP) > 1 and $P < 0.05$.

3 Results

3.1 Network pharmacology analysis

3.1.1 The identification of chemical compounds and potential targets for FFEJJ on AA A total of 301 chemical compounds in FFEJJ were identified from the TCMSP, TCMIP, and BATMAN-TCM databases. Among them, 74 chemical compounds were present in Hongshen (Ginseng Radix et Rhizoma Rubra), 76 in Shudihuang (Rehmanniae Radix Preparata), 134 in Dangshen (Codonopsis Radix), and 32 in Shanzha (Crataegi Fructus). Of the 301 chemical compounds, we further screened 22 active components that conformed to OB ⩾ 30% and DL ⩾ 0.18 (Table 1). In addition, 17 amino acids in Ejiao (Asini Corii Colla) were identified using PubMed. Four chemical compounds, including arginine, histidine, lysine, and threonine, were taken into account in the network pharmacology analysis [19-22]. According to previous study, four compounds (including panaxynol, ginsenoside rf, ginsenoside rh2, and panaxydol) in Hongshen (Ginseng Radix et Rhizoma Rubra) were also selected as presumptive active components [23]. For the 30 active components in FFEJJ, the TCMSP and UniProt databases were used to identify 138 protein targets. Among these targets, 21 were related to Hongshen (Ginseng Radix et Rhizoma Rubra), 39 to Ejiao (Asini Corii Colla), 26 to Shudihuang (Rehmanniae Radix Preparata), 91 to Dangshen (Cadonopsis Radix), and 21 to Shanzha (Crataegi Fructus). The details are listed in Table 2. A total of 238 targets and 651 targets for AA were identified using the DisGeNET and GeneCards databases, respectively. There were 133 overlapping targets in the above two databases. Consequently, after eliminating redundancy, 24 targets were found to be related to the 30 active components in FFEJJ and were associated with AA.

Table 1 Compounds information of FFEJJ

Source	Mol ID	Molecule Name	MW	OB (%)	DL	Database
Dangshen (Cadonopsis Radix)	MOL008407	Stigmasterone	410.75	45.40	0.76	TCMSP
	MOL008411	11-Hydroxyrankinidine	356.46	40.00	0.66	TCMSP
	MOL007059	3-Beta-hydroxymethy llenetanshiquinone	294.32	32.16	0.41	TCMSP
	MOL008393	7-(beta-Xylosyl)cephalomannine_qt	830.02	38.33	0.29	TCMSP
	MOL003896	7-Methoxy-2-methyl isoflavone	266.31	42.56	0.20	TCMSP
	MOL008397	Daturilin	436.64	50.37	0.77	TCMSP
	MOL002879	Diop	390.62	43.59	0.39	TCMSP
	MOL005321	Frutinone A	264.24	65.9	0.34	TCMSP
	MOL008400	Glycitein	284.28	50.48	0.24	TCMSP, TCMIP
	MOL000006	Luteolin	286.25	36.16	0.25	TCMSP, TCMIP
	MOL007514	Methyl icosa-11,14-dienoate	322.59	39.67	0.23	TCMSP
	MOL002140	Perlolyrine	264.3	65.95	0.27	TCMSP, TCMIP
	MOL001006	Poriferasta-7,22E-dien-3beta-ol	412.77	42.98	0.76	TCMSP
	MOL006774	Stigmast-7-enol	414.79	37.42	0.75	TCMSP
	MOL003036	ZINC03978781	412.77	43.83	0.76	TCMSP
Hongshen (Ginseng Radix et Rhizoma Rubra)	MOL012330	Ginsenoside rf	801.14	17.74	0.24	TCMSP, TCMIP
	MOL012332	Ginsenoside rh2	622.98	36.32	0.56	TCMSP, TCMIP
	MOL012334	Panaxydol	260.41	61.67	0.13	TCMSP, TCMIP
	MOL012328	Panaxynol	244.41	42.44	0.10	TCMSP, TCMIP
Shudihuang (Rehmanniae Radix Preparata)	MOL001987	β-Sitosterol	546.57	33.94	0.7	TCMSP, BATMAN-TCM
Dangshen (Cadonopsis Radix), Shudihuang (Rehmanniae Radix Preparata), Shanzha (Crataegi Fructus)	MOL004355	Spinasterol	412.77	42.98	0.76	TTCMSP, BATMAN-TCM, TCMIP
	MOL000449	Stigmasterol	412.77	43.83	0.76	TCMSP, BATMAN-TCM, TCMIP

3.1.2 Herbs-components-targets network analysis Our study established an herbs-components-targets (containing 168 nodes and 273 edges) network (Figure 2A) for FFEJJ via Cytoscape. The topological analysis showed that 10 components with degree > 5 were involved in the regulation of multiple targets, including three for flavonoids (luteolin, 7-Methoxy-2-methyl isoflavone, and glycitein), 3 for sterols (stigmasterol, ginsenoside rh2, and ginsenoside rf), and 4 for others (3-beta-hydroxymethyllenetanshiquinone, frutinone A, panaxynol, and panaxydol). These findings suggest that FFEJJ works through multiple components and targets.

3.1.3 PPI network Repetitive targets between the GeneCards and the DisGeNET databases were excluded, and 756 AA-correlated targets were collected. To identify the targets with essential contributions,

Table 2 Herb-compound-active components-potential targets for FFEJJ

Herb	Number of compounds	Number of active components	Number of potential targets
Ejiao (Asini Corii Colla)	17	4	39
Hongshen (Ginseng Radix et Rhizoma Rubra)	74	7	21
Shudihuang (Rehmanniae Radix Preparata)	76	2	26
Dangshen (Cadonopsis Radix)	134	21	91
Shanzha (Crataegi Fructus)	32	6	21

we imported the 24 co-targets of FFEJJ-AA and constructed FFEJJ-AA PPI networks via STRING (Figure 2B and 2C). Our PPI network showed that the top five proteins most closely associated with the anti-AA effects of FFEJJ were VEGFA, AKT1, IL-6, CASP3, and ICAM1, which conformed to the results of previous animal experiments (Figure 2D).

3.1.4 GO analysis and KEGG pathway enrichment analysis The DAVID platform was used to investigate the biological processes and functions of the candidate targets of FFEJJ with respect to AA. In this study, 24 co-targets were annotated by GO function analysis and KEGG pathway analysis. A total of 30 GO terms are displayed in Figure 3, including biological processes (BP), cellular components (CC), and molecular function (MF). The top five enriched GO terms for FFEJJ (Figure 3A) indicate that FFEJJ elicited its anti-AA effects through the following pathways: negative regulation of the apoptotic process, response to drug, positive regulation of chemokine biosynthetic process, positive regulation of nitric oxide biosynthetic process, and positive regulation of

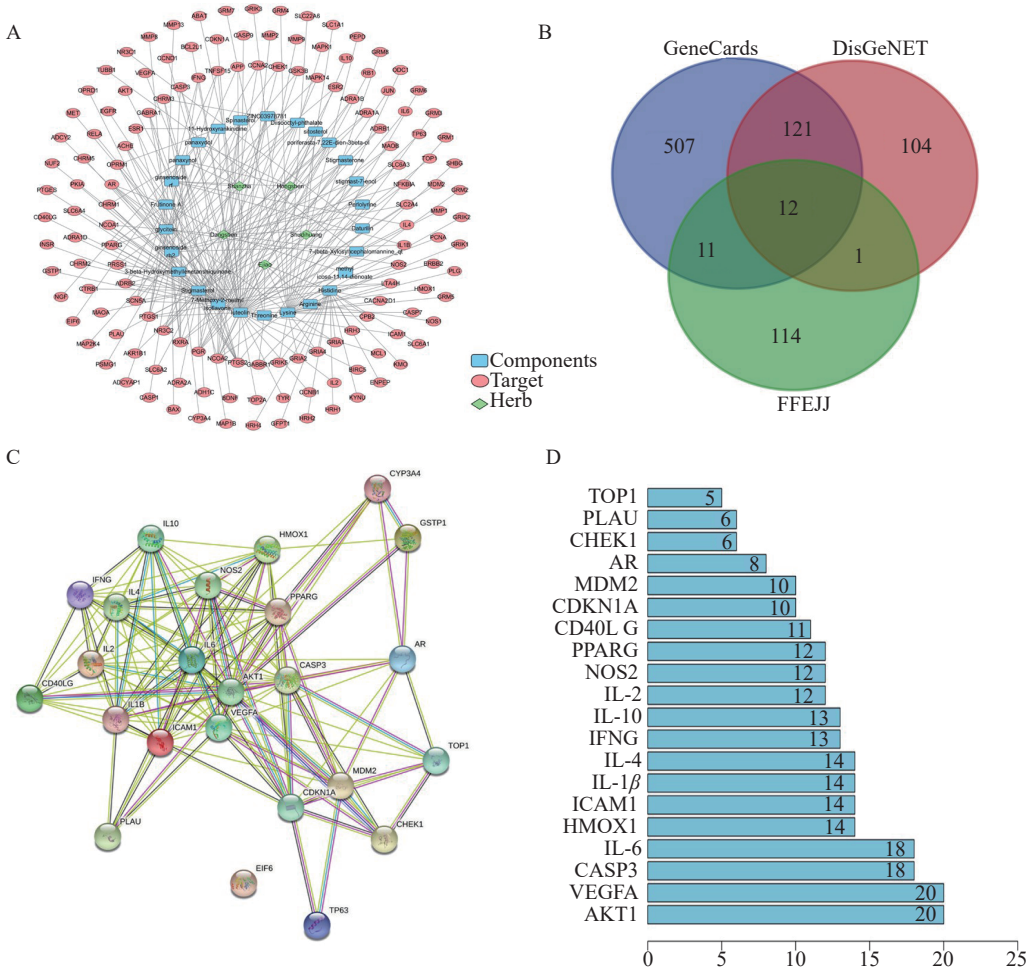

Figure 2 Network pharmacology analysis for FFEJJ

A, herb-components-targets network of FFEJJ. B, targets Venn diagram of FFEJJ against AA. C, PPI network of FFEJJ and AA. D, target count of top 20 in PPI network.

sequence-specific DNA binding transcription factor activity.

Pathway enrichment was conducted to clarify the activities of FFEJJ. The top 13 KEGG pathways (Figure 3B and 3C) with $P < 0.05$ were identified for FFEJJ, including immune regulation-related pathways (T cell receptor signaling pathway, intestinal immune network for IgA production, Jak-STAT signaling pathway, and Toll-like receptor signaling pathway), inflammatory regulatory corelated pathways (TNF signaling pathway, PI3K-Akt signaling pathway, NF-kappa B signaling pathway), hematopoiesis-related pathways (osteoclast differentiation, hematopoietic cell lineage), oxidative stress-related pathways (HIF-1 signaling pathway, FoxO signaling pathway), and other pathways (cytokine-cytokine receptor interaction, p53 signaling pathway). In summary, these results suggest that FFEJJ exerts an anti-AA effect by combining effective targets with various bioactivities pathways. Pathway information is presented in Table 3.

3.2 Serum metabolomic analysis

3.2.1 Metabolic profiles Serum metabolomics analysis was conducted to further characterize the metabolite changes in AA rats, and the functional activities of FFEJJ were verified via metabolic profiles. According to the HMDB and Mrtlin platforms, 895 and 610 endogenous metabolites were identified in the positive and negative ion modes, respectively.

HCA is described as a probe tool that distinguishes natural groups and associates similar classes in a batch of data. As shown in Figure 4, the AA model group were briefly separated from the control group, indicating that APH combined with CTX caused a serious metabolic disorder in rats. Compared with the model group, animals treated with FFEJJ showed a trend towards the control group, suggesting that FFEJJ can regulate the metabolic disorder caused by AA (Figure 4A). In addition, OPLS-DA, a supervised analysis strategy, was used to screen

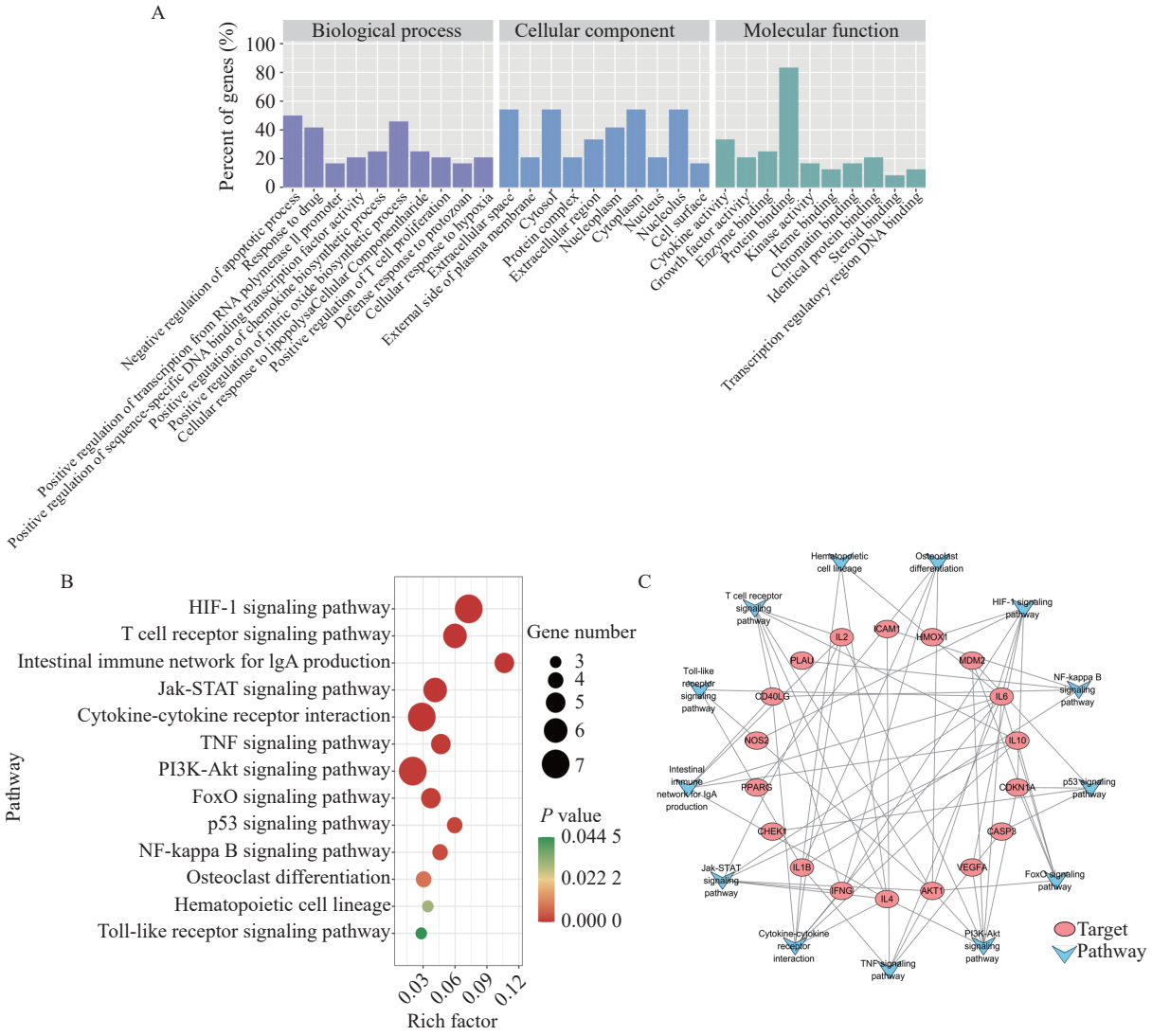

Figure 3 Enrichment analysis for FFEJJ on AA

A, GO analysis. B, KEGG pathway analysis. C, target-pathway network of FFEJJ on treating AA.

Table 3 The top 13 KEGG pathways associated with FFEJJ in relation to AA

KEGG ID	Pathway	*P* value	Target
map04066	HIF-1 signaling pathway	0.000 000 3	IL-6, CDKN1A, IFNG, NOS2, HMOX1, AKT1, VEGFA
map04660	T cell receptor signaling pathway	0.000 012	IL-10, IL-4, CD40LG, IFNG, AKT1, IL-2
map04672	Intestinal immune network for IgA production	0.000 012	IL-10, I-L4, IL-6, CD40LG, IL-2
map04630	Jak-STAT signaling pathway	0.000 077	IL-10, IL-4, IL-6, IFNG, AKT1, IL-2
map04060	Cytokine-cytokine receptor interaction	0.000 085	IL-10, IL-4, IL-6, CD40LG, IFNG, IL-1β, IL-2
map04668	TNF signaling pathway	0.000 326	IL-6, IL-1β, CASP3, AKT1, ICAM1
map04151	PI3K-Akt signaling pathway	0.000 573	IL-4, IL-6, CDKN1A, MDM2, AKT1, IL-2, VEGFA
map04068	FoxO signaling pathway	0.000 767	IL-10, IL-6, CDKN1A, MDM2, AKT1
map04115	p53 signaling pathway	0.001 191	CDKN1A, CASP3, CHEK1, MDM2
map04064	NF-kappa B signaling pathway	0.002 529	CD40LG, PLAU, IL-1β, ICAM1
map04380	Osteoclast differentiation	0.007 977	IFNG, IL-1β, AKT1, PPARG
map04640	Hematopoietic cell lineage	0.031 004	IL-4, IL-6, IL-1β
map04620	Toll-like receptor signaling pathway	0.044 473	IL-6, IL-1β, AKT1

and identify the differential metabolites responsible for class separation. OPLS-DA scoring showed good division between groups (Figure 4B). Endogenous metabolites with fold change (FC) > 2 or FC < 0.5, and $P < 0.05$, were regarded as potential biomarkers. Based on the positive and negative ion modes, 423 biomarkers (58 upregulated and 365 downregulated) were identified between the control and model groups. Similarly, 79 biomarkers (15 upregulated and 64 downregulated) were identified as differential metabolites between the FFEJJ and model groups (Figure 5A and 5B).

Furthermore, to develop our understanding of the regulation rules for FFEJJ, 35 overlapping altered metabolites were identified, and the metabolic profiles are shown in the heat map (Figure 5C and 5D). Notably, FFEJJ reversed 26 metabolites compared to rats without treatment (Table 4).

3.2.2 Metabolic pathway analysis Enrichment analysis for biomarkers was performed to reveal the correlative metabolic pathways and function and illustrate the potential mechanisms underlying the therapeutic effects of FFEJJ at the metabolic level. Overall, 423 biomarkers were altered in the control and AA models enriched in 24 metabolic pathways. Similarly, 79 metabolites with significant changes between FFEJJ therapy and the AA model were involved in 11 metabolic pathways. Moreover, 10 overlapping metabolic pathways were observed between the control vs. model and FFEJJ vs. model groups. Among them, five metabolic pathways with impact >0.1 were considered key metabolic pathways for FFEJJ in the treatment of AA, including retinol metabolism, sphingolipid metabolism, pentose and glucoronate interconversions, glycerophospholipid metabolism, and arachidonic acid metabolism, which may also be responsible for the metabolic changes in AA rats (Figure 6).

Sphingolipids (C00319) and sphinganine (C00836) are affected by sphingolipid metabolism. PC [15∶0/20∶3 (8Z, 11Z, 14Z)] (C00157) and LysoPC [22∶1 (13Z)] (C04230) were responsible for metabolite nodes in glycerophospholipid metabolism. Arachidonic acid metabolism was regulated by 15(S)-HPETE (C05966) and PC [15∶0/20∶3 (8Z, 11Z, 14Z)] (C00157). In addition, pentose and glucuronate interconversions and retinol metabolism were significantly affected by retinal (C00376) and 6-Hydroxy-5-methoxyindole glucuronide (C03033), respectively. The regulatory effects of FFEJJ are mainly involved in lipid metabolism. In this study, compared to the model group, FFEJJ decreased the serum levels of LysoPC [P-18∶1 (9Z)] ($P < 0.001$), LysoPC [20∶1 (11Z)], LysoPC [22∶1 (13Z)], and LysoPC(P-18∶0) ($P < 0.05$), while it increased PC [16∶0/16∶1 (9Z)] ($P < 0.01$). In addition, FFEJJ decreased the sphinganine ($P < 0.001$) and cer (d18∶1/2∶0) ($P < 0.05$), while it upregulated the level of S1P ($P<0.05$). Our results suggest that FFEJJ is involved in the regulation of sphingolipid metabolism via multiple metabolites.

4 Discussion

AA is considered a fatal blood disease that can occur at any age and is more prevalent in Asia [24]. TCMs comprise a combination of multi-flavored herbs and

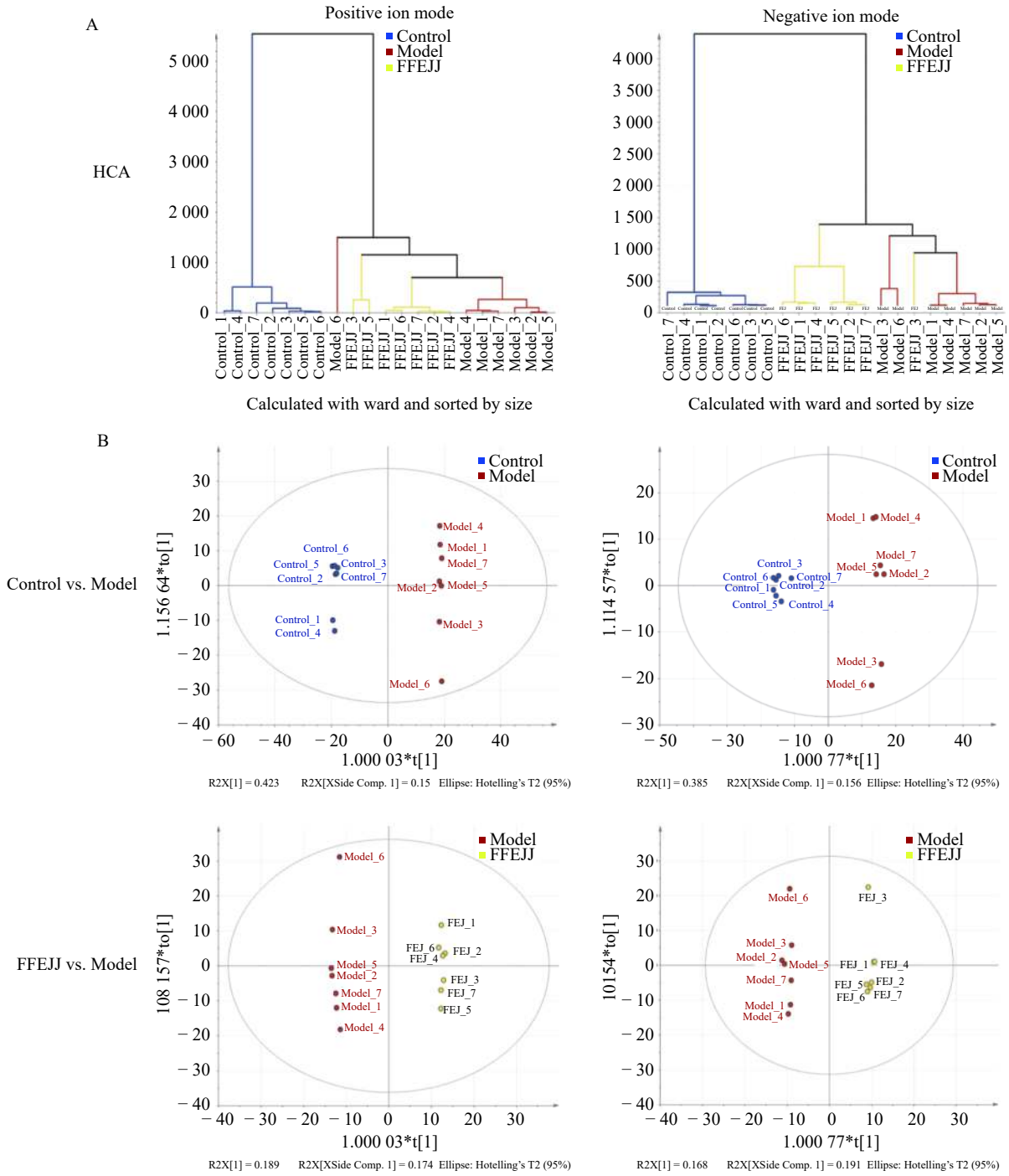

Figure 4 Multivariate statistical analysis of control vs. model and FFEJJ vs. model
A,HCA analysis. B, OPLS-DA score plots.

are considered to be effective for bone marrow failure-related diseases, and has the characteristics of high safety, low toxicity, and fewer side effects. Network pharmacology and associated databases were used to forecast the dominant targets of FFEJJ on AA. The development of network pharmacology, containing herbs, ingredients, and disease platforms, has accelerated the advancement of approaches employed to reveal the bioactive constituents and underlying mechanisms of TCMs [25].

Luteolin and ginsenosides were identified in this study. Previous studies showed that luteolin alleviates HgCl2-induced AA by regulating the Sirt1/Nrf2/TNF-α signaling pathway [26, 27]. Accumulating evidence indicates that ginsenosides might be an alternative strategy for the treatment of myelosuppression induced by chemotherapy or radiotherapy [23]. In addition, ginsenosides possess dual activities in AA, restoring hematopoiesis and regulating immunity [28]. These studies indicate that FFEJJ has the advantages of multiple components and multiple targets in the treatment of AA. Network pharmacology analysis

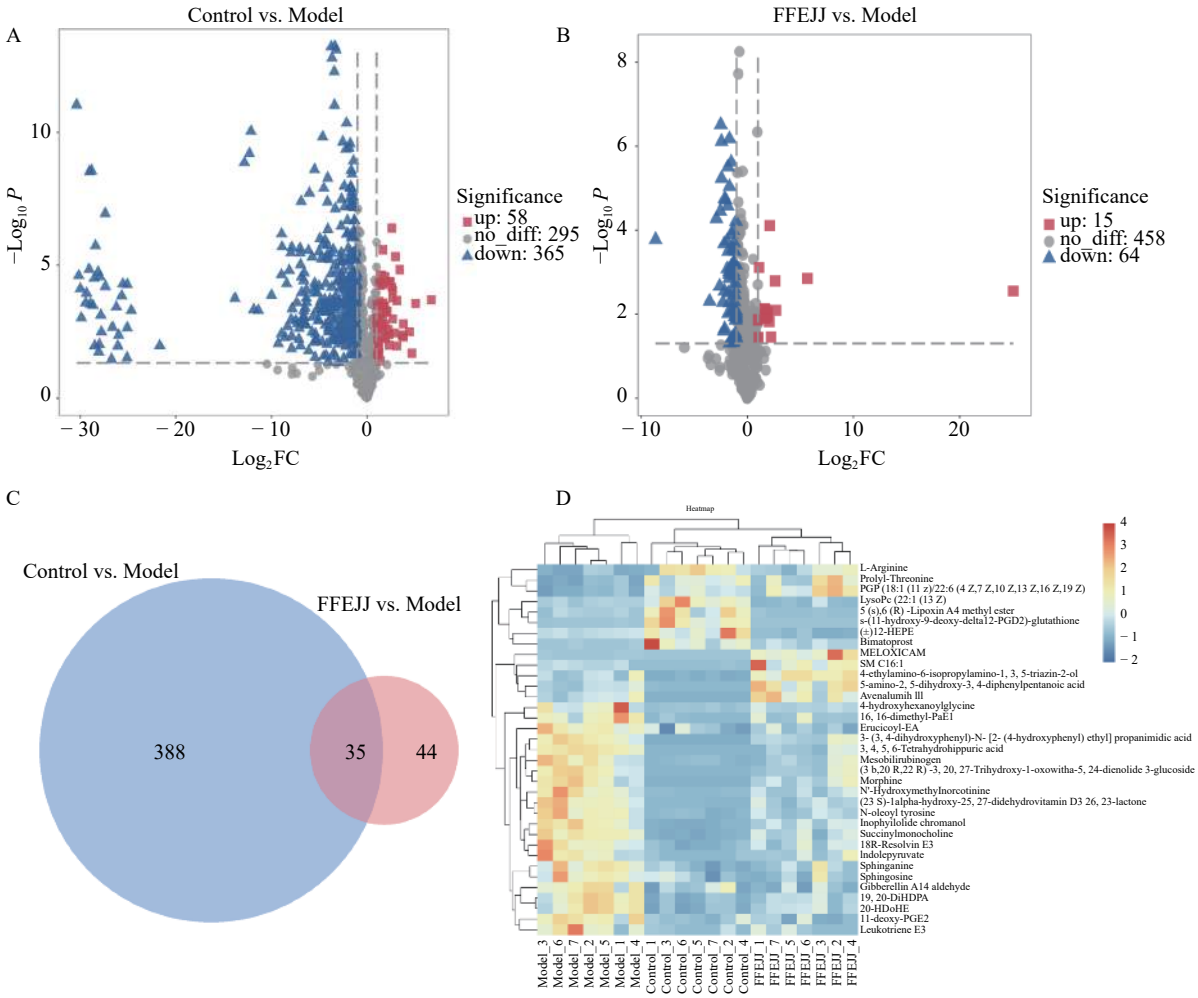

Figure 5 Differential metabolites analysis of control vs. model and FFEJJ vs model

A,volcano diagram of control vs. model groups. B, volcano diagram of FFEJJ vs. model groups. C, the veen diagram of differential endogenous metabolites. D, heat map of the 35 overlap biomarkers.

Table 4 Differentially expressed endogenous metabolites of 35 overlapping biomarkers between the control vs. model and FFEJJ vs. model groups

Metabolite	Control vs. model group			FFEJJ vs. model group		
	Trend	FC	VIP	Trend	FC	VIP
Bimatoprost	↑*	25.929 260	1.402 65	↑#	4.728 753	1.606 70
L-arginine	↑**	6.529 770	1.198 77	↑##	3.727 558 0	1.543 02
Prolyl-threonine	↑***	6.124 221	1.329 63	↑##	6.454 493	1.558 48
PGP [18∶1 (11Z)/22∶6 (4Z, 7Z, 10Z, 13Z, 16Z, 19Z)]	↑***	3.748 950	1.423 19	↑##	6.129 689	1.686 52
Sphingosine	↓**	0.455 488	1.092 34	↓#	0.480 865	1.508 87
Gibberellin A14 aldehyde	↓**	0.444 137	1.079 20	↓###	0.344 406	1.827 31
Erucicoyl-EA	↓***	0.387 618	1.234 14	↓###	0.426 410	1.926 48
11-Deoxy-PGE2	↓***	0.327 019	1.267 23	↓###	0.284 707	1.892 20
Sphinganine	↓***	0.274 168	1.309 65	↓##	0.491 555	1.529 08
4-Hydroxyhexanoylglycine	↓*	0.219 752	1.009 14	↓#	0.407 118	1.258 92
18R-Resolvin E3	↓***	0.188 058	1.282 00	↓#	0.490 375	1.489 31

Table 4 Continued

Metabolite	Control vs. model group			FFEJJ vs. model group		
	Trend	FC	VIP	Trend	FC	VIP
Mesobilirubinogen	↓***	0.177 034	1.274 84	↓#	0.432 845	1.503 32
19,20-DiHDPA	↓***	0.166 015	1.345 75	↓###	0.399 679	1.801 18
20-HDoHE	↓***	0.142 311	1.326 45	↓##	0.428 339	1.706 70
Succinylmonocholine	↓***	0.100 378	1.473 79	↓###	0.444 297	1.891 73
Leukotriene E3	↓**	0.086 765	1.061 61	↓#	0.229 059	1.393 53
N-oleoyl tyrosine	↓***	0.078 383	1.260 34	↓##	0.306 406	1.158 37
Inophyllolide chromanol	↓***	0.065 110	1.400 85	↓##	0.428 732	1.780 06
(23S)-1Alpha-hydroxy-25,27-didehydrovitamin D3 26,23-lactone	↓***	0.050 390	1.342 23	↓##	0.308 168	1.766 08
Indolepyruvate	↓**	0.048 754	1.163 53	↓#	0.361 233	1.294 48
N'-Hydroxymethylnorcotinine	↓***	0.047 023	1.288 11	↓##	0.288 736	1.681 16
16,16-Dimethyl-PGE1	↓***	0.034 309	1.244 88	↓##	0.286 941	1.128 11
Morphine	↓***	0.022 421	1.327 99	↓##	0.358 020	1.549 30
3-(3,4-Dihydroxyphenyl)-N-[2-(4-hydroxyphenyl)ethyl]propanimidic acid	↓***	0.002 107	1.424 88	↓##	0.443 507	1.667 74
(3b,20R,22R)-3,20,27-Trihydroxy-1-oxowitha-5,24-dienolide 3-glucoside	↓***	0.000 070	1.313 79	↓#	0.459 267	1.290 18
3,4,5,6-Tetrahydrohippuric acid	↓***	0.000 001	1.501 11	↓###	0.245 892	2.054 73
(±)12-HEPE	↑*	2.169 601	1.410 34	↓###	0.312 138	1.624 65
4-Ethylamino-6-isopropylamino-1,3,5-triazin-2-ol	↓**	0.307 291	1.082 48	↑###	2.173 343	1.822 86
5(S),6(R)-Lipoxin A4 methyl ester	↑**	7.370 820	1.111 25	↓##	0.085 451	1.624 16
5-Amino-2,5-dihydroxy-3,4-diphenylpentanoic acid	↓**	0.008 361	1.175 00	↑##	3.290 601	1.563 09
Avenalumin III	↓***	0.019 856	1.208 06	↑#	2.098 719	1.304 72
LysoPC[22∶1 (13Z)]	↑**	3.775 989	1.496 23	↓#	0.496 587	1.904 69
Meloxicam	↓*	0.000 003	1.013 79	↑##	50.623 910	1.766 36
S-(11-Hydroxy-9-deoxy-delta12-PGD2)-glutathione	↑***	34.542 79	1.427 08	↓###	0.002 514	1.703 62
SM C16∶1	↓***	0.034 294	1.279 17	↑#	4.225 029	1.461 91

*$P < 0.05$, **$P < 0.01$, and ***$P < 0.001$, compared with normal control group; #$P < 0.05$, ##$P < 0.01$, and ###$P < 0.001$, compared with model group.

plays an important role in clarifying this complex relationship by linking the chemical space of components with biomolecules. The upregulation of VEGFA accelerates the process of anemia, whereas the upregulation of adhesive molecules in bone marrow mesenchymal stem cells (BMMSCs), such as VLA-4, VCAM-1, and ICAM-1, participates in AA protection [29, 30]. CASP3 overexpression occurs during erythropoietic stress, especially under conditions of tissue hypoxia during the period of anemia [31]. Research demonstrates that irradiation and chemotherapeutic drugs increase IL-6 expression in AA, which may disturb the balance of the bone marrow hematopoietic microenvironment [32]. Our study found that luteolin in Dangshen (Codonopsis Radix) is capable of concurrently regulating VEGFA, AKT1, CASP3, and ICAM1. Panaxytol, ginsenoside rh2, and luteolin synergistically regulated CASP3. Network

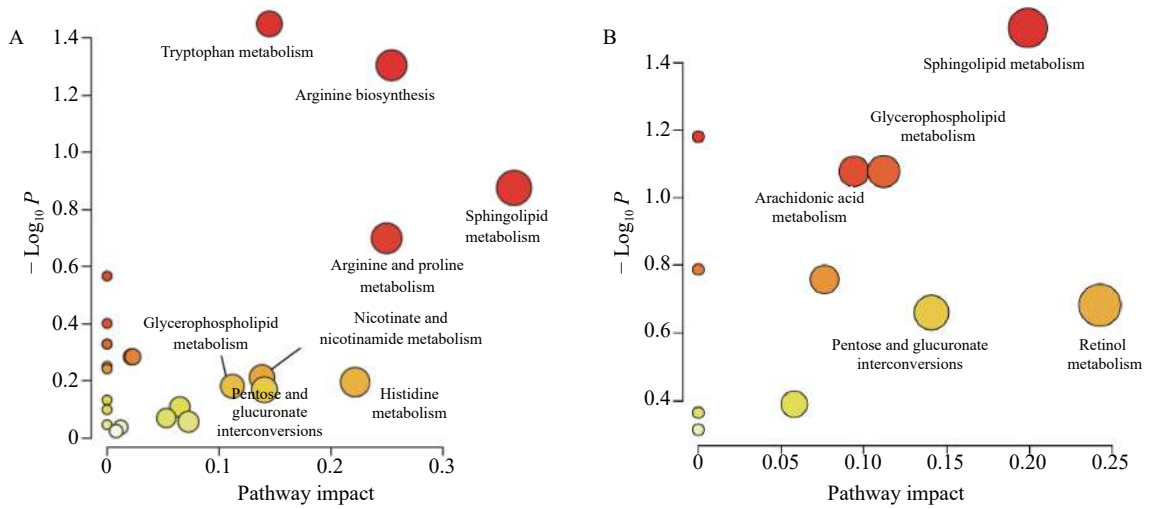

Figure 6 Metabolic pathway analysis

A, eleven metabolic pathways enriched in the model group. B, five metabolic pathways enriched in the FFEJJ group.

pharmacology suggests that it is possible to analyze complex systems and establish relationships between multiple targets in the chemical compounds of TCM and specific diseases. According to our results, FFEJJ may be involved in regulating bone marrow hematopoietic microenvironment-related targets to achieve the therapeutic effect of AA.

It has been demonstrated that lipid metabolism is a vital aspect of hematopoiesis in the cell-autonomous and bone marrow (BM) microenvironment [33]. A previous study showed that the levels of lysophosphatidylcholines (lysoPCs) containing lysoPC (18∶0), lysoPC (20∶4), lysoPC (16∶0), lysoPC (18∶2), sphinganine, thiamine pyrophosphate, phytosphingosine, and glycerophosphocholine increased significantly in hemolytic and AA rats [34]. PCs are the precursors of lysoPC and a primary constituent of membrane lipids. During terminal erythropoiesis, the levels of PC and phosphocholine are decreased and metabolized to choline [35]. In addition, PC also serves as a substrate reservoir for polyunsaturated fatty acids, such as eicosanoids and hydroxyeicosatetraenoic acid (HETE). HETE participates in bone marrow repopulation and limits the self-renewal of long-term hematopoietic stem cell (LT-HSC) [33]. 15-HETE is produced in erythroid progenitor cells when treated with erythropoietin [36]. The 15(S)-HPETE inhibits the TNF-α-triggered expression of adhesion molecules, including intercellular adhesion molecule-1 (ICAM-1) and vascular cell adhesion molecule-1 (VCAM-1), which partly conforms to the results of the network pharmacology analysis [37]. Thus, FFEJJ may alleviate AA by maintaining the BM microenvironment.

Sphingolipids play important roles in membrane integrity and cellular signaling. Ceramide and sphingosine-1-phosphate (S1P) are two types of central bioactive lipids associated with sphingolipids. S1P has been shown to trigger CXCL12 secretion from mesenchymal stem cells, thereby increasing the excretion of progenitor cells via a reactive oxygen species (ROS)-dependent pathway and modulating hematopoiesis [38, 39]. Our results suggest that FFEJJ is involved in the regulation of sphingolipid metabolism via multiple metabolites.

Changes in amino acids are also one of the causes for hematopoietic dysfunction [40]. Previous studies have shown that Ejiao (Asini Corii Colla) can regulate the metabolism of arginine and threonine and participate in the treatment of diseases [41, 42]. Our results showed that FFEJJ can increase serum levels of L-arginine and prolyl-threonine in anemia and improve the symptoms of aplastic anemia. It is suggested that Ejiao (Asini Corii Colla) , as a blood-enriching component of FFEJJ, may play an important role in regulating the metabolism of organisms.

This study focused on the relationship between metabolites and targets regulated by active components. Network pharmacology combined with metabolomic analyses was used to investigate this correlation. In addition, two crucial pathways, hematopoiesis -related pathways and hematopoietic microenvironment-related pathways, were enriched. Among them, luteolin, ginsenoside rh2, and panaxytol were the hub active components of FFEJJ. Ginsenoside Rh2 is involved in the regulation of VEGFA and CASP3 [43, 44]. Luteolin can decrease the expression of ICAM1 and CASP3 [45, 46]. Panaxytol normalizes CASP3 expression [47]. This is consistent with our prediction of the interaction network. In addition, these three targets are responsible for maintaining the stability of the BM microenvironment and regulating hematopoi esis. Lipid metabolism (including HETE, Lyso PCs, and S1P) is the main metabolic regulatory pathway

altered by FFEJJ. Normalization of lipid metabolism is an important aspect in maintaining hematopoiesis. he above pathways partly account for the protective mechanism of FFEJJ against AA. Moreover, the results indicate that FFEJJ has an impact on network regulation through the synergistic action of multiple components on multiple targets, thus playing an important role in the treatment of AA (Figure 7).

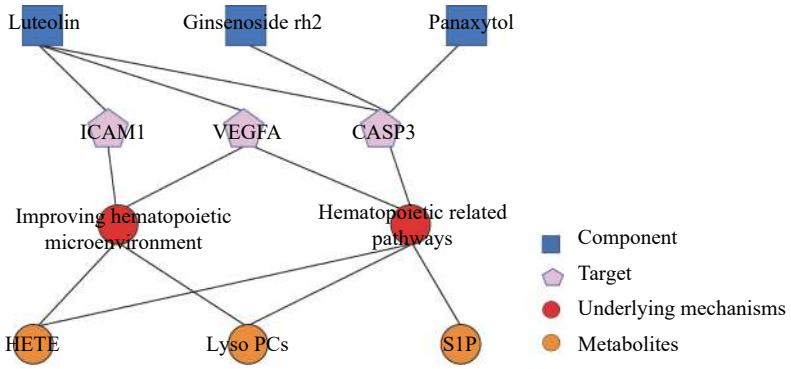

Figure 7 Interaction network of components, metabolites, targets, and the mechanisms regulated by FFEJJ in treating AA

5 Conclusion

In summary, network pharmacology combined with serum metabolomics showed that FFEJJ provided protection against AA via a target network and multiple pathways. Three hub compounds (luteolin, ginsenoside rh2, and panaxytol) and three key targets (VEGFA, CASP3, and ICAM1) responsible for maintaining the stability of hematopoietic cells and for supporting bone marrow hematopoiesis were identified. The integrated network also revealed that metabolic regulation by FFEJJ, particularly lipid metabolism, is an important part of its anti-AA activity. These results suggest that FFEJJ may be a new treatment option for AA. Moreover, the emergence of network pharmacology integrated metabolomics makes it possible to analyze TCM from a systems perspective and at the molecular level.

Acknowledgements

We thank for the funding support from the Natural Science Foundation of China (No. 81673585, No. 81874493, No. 81573956); Program of Survey of Chinese Medicines of China (No. [2017]66), Science Foundation of Hunan Province (No. 2019JJ50345, No. 2020JJ5325, No. 2021168), Key Research and Development Project of Changsha Science and Technology (No. kq1901067); Training Program for Excellent Young Innovators of Changsha (No. kq1802017); Research on the Comprehensive Development and Utilization of Characteristic Traditional Chinese Medicine Resources (No. 2060302); and the Support of Hunan Province Traditional Chinese Medicine Preparation and Quality Traceability Engineering and Technology Center, and the 2011 Collaboration and Innovation Center for Digital Chinese Medicine in Hunan.

Competing interests

The authors declare no conflict of interest.

References

[1] YOUNG NS. Aplastic Anemia. The New England Journal of Medicine, 2018, 379(17): 1643–1656.
[2] AHMED P, CHAUDHRY QUN, SATTI TM, et al. Epidemiology of aplastic anemia: a study of 1 324 cases. Hematology, 2020, 25(1): 48–54.
[3] YOUNG NS, KAUFMAN DW. The epidemiology of acquired aplastic anemia. Haematologica, 2008, 93(4): 489–492.
[4] WU Z, MIAO M, QIU Y, et al. Association between polymorphisms in PDCD1 gene and aplastic anemia in Chinese Han population. Leuk Lymphoma, 2013, 54(10): 2251–2254.
[5] PESLAK SA, OLSON T, BABUSHOK DV. Diagnosis and treatment of aplastic anemia. Current Treatment Options in Oncology, 2017, 18(12): 70.
[6] ZHU C, GAO Y, JIANG T, et al. Meta-analysis of Huangqi injection for the adjunctive therapy of aplastic anemia. International Journal of Clinical and Experimental Medicine, 2015, 8(7): 10256–10264.
[7] ZHANG Y, YE T, HONG Z, et al. Pharmacological and transcriptome profiling analyses of Fufang E'jiao Jiang during chemotherapy-induced myelosuppression in mice. Journal of Ethnopharmacology, 2019, 238: 111869.
[8] LI X, ZHANG Y, HONG Z, et al. Transcriptome profiling analysis reveals the potential mechanisms of three bioactive ingredients of Fufang E'jiao Jiang during chemotherapy-induced myelosuppression in Mice. Frontiers in Pharmacology, 2018, 9: 616.
[9] LI S, ZHANG B. Traditional Chinese medicine network pharmacology: theory, methodology and application. Chinese Journal Natural Medecines, 2013, 11(2): 110–120.
[10] PANG HQ, YUE SJ, TANG YP, et al. Integrated metabolomics and network pharmacology approach to explain possible action mechanisms of Xin-Sheng-Hua Granule for treating anemia. Frontiers in Pharmacology, 2018, 9: 165.
[11] HUA YL, MA Q, YUAN ZW, et al. A novel approach based

on metabolomics coupled with network pharmacology to explain the effect mechanisms of Danggui Buxue Tang in anaemia. Chinese Journal of Nature Medicines, 2019, 17(4): 275–290.
[12] DU Q, HE D, ZENG HL, et al. Siwu paste protects bone marrow hematopoietic function in rats with blood deficiency syndrome by regulating TLR4/NF-κB/NLRP3 signaling pathway. Journal of Ethnopharmacology, 2020, 262: 113160.
[13] LI S, LIN H, QU C, et al. Urine and plasma metabonomics coupled with UHPLC-QTOF/MS and multivariate data analysis on potential biomarkers in anemia and hematinic effects of herb pair Gui-Hong. Journal of Ethnopharmacology, 2015, 170: 175–183.
[14] HUANG JH, HE D, CHEN L, et al. GC-MS based metabolomics strategy to distinguish three types of acute pancreatitis. Pancreatology, 2019, 19(5): 630–637.
[15] WISHART DS, FEUNANG YD, MARCU A, et al. HMDB 4.0: the human metabolome database for 2018. Nucleic Acids Research, 2018, 46(D1): D608-D617.
[16] GUIJAS C, MONTENEGRO-BURKE JR, DOMINGO-ALMENARA X, et al. Metlin: a technology platform for identifying knowns and unknowns. Analytical Chemistry, 2018, 90(5): 3156–3164.
[17] ROCHA WFC, SHEEN DA, BEARDEN DW. Classification of samples from NMR-based metabolomics using principal components analysis and partial least squares with uncertainty estimation. Analytical and Bioanalytical Chemistry, 2018, 410(24): 6305–6319.
[18] YANG Q, LIN SS, YANG JT, et al. Detection of inborn errors of metabolism utilizing GC-MS urinary metabolomics coupled with a modified orthogonal partial least squares discriminant analysis. Talanta, 2017, 165: 545–552.
[19] FENG RN, NIU YC, SUN XW, et al. Histidine supplementation improves insulin resistance through suppressed inflammation in obese women with the metabolic syndrome: a randomised controlled trial. Diabetologia, 2013, 56(5): 985–994.
[20] MALINOVSKY AV. Reason for indispensability of threonine in humans and other mammals in comparative aspect. Biochemistry (Mosc), 2017, 82(9): 1055–1060.
[21] MARTIN S, DESAI K. The effects of oral arginine on its metabolic pathways in Sprague-Dawley rats. The British Journal of Nutrition, 2020, 123(2): 135–148.
[22] SATO T, ITO Y, NAGASAWA T. Regulation of skeletal muscle protein degradation and synthesis by oral administration of lysine in rats. Journal of Nutritional Science and Vitaminology (Tokyo), 2013, 59(5): 412–419.
[23] HE M, WANG N, ZHENG W, et al. Ameliorative effects of ginsenosides on myelosuppression induced by chemo therapy or radiotherapy. Journal of Ethnopharmacology, 2021, 268: 113581.
[24] CHIU ML, HSU YL, CHEN CJ, et al. Chinese herbal medicine therapy reduces the risks of overall and anemia-related mortalities in patients with aplastic anemia: a nationwide retrospective study in taiwan. Frontiers in Pharmacology, 2021, 12: 730776.
[25] LIU XJ, WANG YZ, WEI FX, et al. The synergistic anti-depression effects of different efficacy groups of Xiaoyaosan as demonstrated by the integration of network pharmacology and serum metabolomics. Journal of Pharmaceutical and Biomedical Analysis, 2021, 197: 113949.
[26] TAN X, LIU B, LU J, et al. Dietary luteolin protects against HgCl(2)-induced renal injury via activation of Nrf2-mediated signaling in rat. Journal of Inorganic Biochemistry, 2018, 179: 24–31.
[27] YANG D, TAN X, LV Z, et al. Regulation of Sirt1/Nrf2/TNF-α signaling pathway by luteolin is critical to attenuate acute mercuric chloride exposure induced hepatotoxicity. Scientific Reports, 2016, 6: 37157.
[28] ZHENG ZY, YU XL, DAI TY, et al. Panaxdiol saponins component promotes hematopoiesis and modulates lymphocyte dysregulation in aplastic anemia model mice. Chinese Journal of Integrative Medicine, 2019, 25(12): 902–910.
[29] YANG J, ZHANG L, WANG H, et al. Protective effects of chronic intermittent hypobaric hypoxia pretreatment against Aplastic Anemia through improving the adhesiveness and stress of mesenchymal stem cells in Rats. Stem Cells International, 2017, 2017: 5706193.
[30] CHONDROU V, KOLOVOS P, SGOUROU A, et al. Whole transcriptome analysis of human erythropoietic cells during ontogenesis suggests a role of VEGFA gene as modulator of fetal hemoglobin and pharmacogenomic biomarker of treatment response to hydroxyurea in β-type hemoglobinopathy patients. Human Genomics, 2017, 11(1): 24.
[31] AISPURU GR, AGUIRRE MV, AQUINO-ESPERANZA JA, et al. Erythroid expansion and survival in response to acute anemia stress: the role of EPO receptor, GATA-1, Bcl-xL and caspase-3. Cell Biology International, 2008, 32(8): 966–978.
[32] CHEN YF, WU ZM, XIE C, et al. Expression level of IL-6 secreted by bone marrow stromal cells in mice with aplastic anemia. ISRN Hematology, 2013, 2013: 986219.
[33] PERNES G, FLYNN MC, LANCASTER GI, et al. Fat for fuel: lipid metabolism in haematopoiesis. Clinical & Translational Immunology, 2019, 8(12): e1098.
[34] LI W, TANG Y, GUO J, et al. Comparative metabolomics analysis on hematopoietic functions of herb pair Gui-Xiong by ultra-high-performance liquid chromatography coupled to quadrupole time-of-flight mass spectrometry and pattern recognition approach. Journal Chromatography A, 2014, 1346: 49–56.
[35] HUANG NJ, LIN YC, LIN CY, et al. Enhanced phosphocholine metabolism is essential for terminal erythropoiesis. Blood, 2018, 131(26): 2955–2966.
[36] BECKMAN BS, MASON-GARCIA M, NYSTUEN L, et al. The action of erythropoietin is mediated by lipoxygenase metabolites in murine fetal liver cells. Biochemical Biophysical Research Communications, 1987, 147(1): 392–398.
[37] HUANG ZH, BATES EJ, FERRANTE JV, et al. Inhibition of stimulus-induced endothelial cell intercellular adhesion molecule-1, E-selectin, and vascular cellular adhesion molecule-1 expression by arachidonic acid and its hydroxy and hydroperoxy derivatives. Circulation Research, 1997, 80(2): 149–158.
[38] ORSINI M, CHATEAUVIEUX S, RHIM J, et al. Sphingolipid-mediated inflammatory signaling leading to autophagy inhibition converts erythropoiesis to myelopoiesis in human hematopoietic stem/progenitor cells. Cell Death and Differentiation, 2019, 26(9): 1796–1812.
[39] GOLAN K, VAGIMA Y, LUDIN A, et al. S1P promotes murine progenitor cell egress and mobilization via S1P1-mediated ROS signaling and SDF-1 release. Blood, 2012, 119(11): 2478–2488.
[40] VAN WASSENHOVE LD, MOCHLY-ROSEN D, WEINBERG KI. Aldehyde dehydrogenase 2 in aplastic anemia, Fanconi anemia and hematopoietic stem cells. Molecular Genetics and Metabolism, 2016, 119(1-2): 28–36.
[41] LIU T, ZHANG P, LING Y, et al. Protective effect of Colla

Corii Asini against lung injuries induced by intratracheal instillation of artificial fine particles in Rats. International Journal of Molecular Sciences, 2018, 20(1): 55.
[42] WANG T, SUN HG, HUA YL, et al. Urine metabonomic study for blood-replenishing mechanism of Angelica sinensis in a blood-deficient mouse model. Chinese Journal of Natural Medicines, 2016, 14(3): 210–219.
[43] LI S, GAO Y, MA W, et al. Ginsenoside Rh2 inhibits invasiveness of glioblastoma through modulation of VEGF-A. Tumour Biology, 2015, 37(1): 15477–15482.
[44] QI Z, LI W, TAN J, et al. Effect of ginsenoside Rh(2) on renal apoptosis in cisplatin-induced nephrotoxicity in vivo. Phytomedicine, 2019, 61: 152862.
[45] HUANG WC, LIOU CJ, SHEN SC, et al. Luteolin attenuates IL-1β-induced THP-1 adhesion to aRPE-19 cells via suppression of NF-κB and MAPK pathways. Mediators of Inflammation, 2020, 2020: 9421340.
[46] ZHANG Y, MA C, LIU C, et al. Luteolin attenuates doxorubicin-induced cardiotoxicity by modulating the PHLPP1/AKT/Bcl-2 signalling pathway. Peer J, 2020, 8: e8845.
[47] YANG ZH, SUN K, YAN ZH, et al. Panaxynol protects cortical neurons from ischemia-like injury by up-regulation of HIF-1alpha expression and inhibition of apoptotic cascade. Chemico Biological Interactions, 2010, 183(1): 165–171.

基于网络药理学和代谢组学的复方阿胶浆抗再生障碍性贫血研究

何丹, 张海潮, 易子漾, 赵荻, 张水寒*

湖南省中医药研究院, 湖南中医药大学, 湖南 长沙 410013, 中国

【摘要】目的 采用网络药理学和血清代谢组学相结合的方法,探讨复方阿胶浆(FFEJJ)治疗再生障碍性贫血(AA)潜在作用机制。**方法** 从中药系统药理学数据库与分析平台(TCMSP),Pubmed,中医药综合药理研究平台(TCMIP),Bioinformatics,中药分子机制的生物信息学分析工具(BATMAN-TCM)用于确定 FFEJJ 的成分和假定的靶点。使用 GeneCard 和 DisGeNET 数据库获得 AA 相关的靶点,构建草药-成分-靶点网络,并分析蛋白质相互作用(PPI)网络,通过京都基因和基因组百科全书(KEGG)对潜在途径进行富集分析。此外,联合乙酰苯肼(APH)和环磷酰胺(CTX)建立 AA 模型评估 FFEJJ 的血液保护作用,基于超高效液相色谱-四极杆飞行时间质谱(UPLC-Q-TOF/MS)的血清代谢组学筛选 FFEJJ 参与抗贫血的潜在代谢标志物和相关代谢途径。**结果** 共筛选 30 个 FFEJJ 活性成分和 24 个与 AA 调控相关的靶点。已报道的 PPI 网络分析显示 VEGFA、AKT1、IL-6、CASP3 和 ICAM1 与 AA 发生发展相关的关键靶点。KEGG 通路富集分析表明, FFEJJ 的假定靶点主要涉及与促进造血和改善造血微环境相关的途径。在对照组和 AA 模型之间鉴定出 423 个代谢物生物标记物,它们参与了 AA 的发展,而 FFEJJ 逆转了 79 种 AA 改变的差异代谢物。KEGG 通路分析表明,FFEJJ 的协同效应主要集中在 24 条代谢途径中,其中,鞘脂代谢、甘油磷脂代谢和花生四烯酸代谢与促进造血和改善造血微环境有关,这与网络药理分析结果一致。3 个关键差异代谢物,羟基二十碳四烯酸(HETE)、1-磷酸鞘氨醇(S1P)和溶血磷脂酰胆碱(lysoPC)与 3 个网络预测靶点 VEGFA、CASP3 和 ICAM1 形成交互网络可能是 FFEJJ 多组分抗 AA 作用的潜在机制。**结论** FFEJJ 是治疗 AA 的一种替代方法,其潜在机制是促进造血和改善造血微环境。本文研究策略提示网络药理学整合代谢组学研究使从系统角度和分子水平阐明中医药作用成为可能。

【关键词】 复方阿胶浆;再生障碍性贫血;网络药理学;代谢组学;脂质代谢;造血微环境;乙酰苯肼;环磷酰胺